NeuroImage: Clinical 23 (2019) 101874

Contents lists available at ScienceDirect

NeuroImage: Clinical

journal homepage: www.elsevier.com/locate/ynicl

Structural magnetic resonance imaging demonstrates abnormal cortical thickness in Down syndrome: Newborns to young adults

Jacob Levman[a,b,c,*], Allissa MacDonald[d], Nicole Baumer[e], Patrick MacDonald[a], Natalie Stewart[a], Ashley Lim[a], Liam Cogger[c], Tadashi Shiohama[a], Emi Takahashi[a,b]

[a] Division of Newborn Medicine, Department of Medicine, Boston Children's Hospital, 401 Park Dr., Boston, MA 02215, USA
[b] Department of Pediatrics, Harvard Medical School, Boston, MA, USA
[c] Department of Mathematics, Statistics and Computer Science, St. Francis Xavier University, Antigonish, NS B2G 2W5, Canada
[d] Department of Biology, St. Francis Xavier University, Antigonish, NS B2G 2W5, Canada
[e] Department of Neurology, Boston Children's Hospital, 300 Longwood Ave, Boston, MA 02115, USA

ARTICLE INFO

Keywords:
Down syndrome
Cortical thickness
Development
Neuroanatomy
Variability

ABSTRACT

Down syndrome (DS) is a genetic disorder caused by an extra copy of all or part of chromosome 21 and is characterized by intellectual disability. We performed a retrospective analysis of 47 magnetic resonance imaging (MRI) examinations of participants with DS (aged 5 to 22 years) and compared them with a large cohort of 854 brain MRIs obtained from neurotypical participants (aged 5 to 32 years) with the objective of assessing the clinical presentation of Down syndrome, towards better understanding the neurological development associated with the condition. An additional cohort of 26 MRI exams from patients with DS and 139 exams from neurotypical participants (aged 0–5 years) are included as part of a supplementary analysis. Regionally distributed cortical thickness measurements, including average measurements as well as standard deviations (intra-regional cortical thickness variability) were extracted from each examination. The largest effect sizes observed were associated with increased average cortical thickness in the postcentral gyrus with specific abnormalities observed in Brodmann's areas 1 and 3b in DS, which was observed across all age ranges. We also observed strong effect sizes associated with decreased cortical thickness variability in the lateral orbitofrontal gyrus, the postcentral gyrus and more in DS participants. Findings suggest regionally irregular gray matter development in DS that can be detected with MRI.

1. Introduction

Down syndrome (DS) has been estimated to occur in approximately 1 in 732 infants in the United States (Sherman et al., 2007). DS is the most common chromosomal disorder in newborns. There are 3 types of DS: trisomy 21 (nondisjunction), translocation and mosaicism. Non-Disjunction Trisomy 21 is the most common type of DS (95% of individuals with DS) with three copies of chromosome 21 in all cells in the body. Translocation, in which part of an extra chromosome 21 attaches to another chromosome, and mosaicism, in which only some cells in the body carry three copies of chromosome 21, rarely occur (Lowry et al., 1976; Nielsen and Sillesen, 1975; Sherman et al., 2007).

Chromosome 21 contains a number of genes, and in DS, gene over expression disrupts numerous processes, including cardiac, digestive, and neural systems which results in characteristic cognitive impairment (Silverman, 2007). Depending on various epigenetic processes across individuals with DS (Jiang et al., 2013; Letourneau et al., 2014), types and severity of cognitive symptoms of DS vary, including problems with learning (Fidler and Nadel, 2007; Wan et al., 2017), memory (Carlesimo et al., 1997; Chapman and Hesketh, 2001; Jarrold et al., 2009), and speech/language (Abbeduto et al., 2007; Jacola et al., 2014) throughout life (Carr, 2005; Couzens et al., 2011). The amyloid precursor protein gene encodes for the amyloid precursor protein (APP) and is located on chromosome 21. The processing of APP generates amyloid beta, the abnormal accumulation of which leads to amyloid plaques (Folin et al., 2003), which causes early onset Alzheimer's disease (AD) with further cognitive impairment in individuals with DS (Annus et al., 2016; Hamlett et al., 2018; Head et al., 2012; Lao et al., 2017; Rafii et al., 2017; Raha-Chowdhury et al., 2018). Research has shown that virtually all adults with DS have amyloid beta plaques and neurofibrillary tangles for a neuropathological diagnosis of AD, with a high proportion of these individuals developing dementia and

* Corresponding author at: Boston Children's Hospital, Harvard Medical School, 401 Park Dr. Boston, MA 02215, USA.
E-mail address: jacob.levman@childrens.harvard.edu (J. Levman).

https://doi.org/10.1016/j.nicl.2019.101874
Received 23 October 2018; Received in revised form 17 May 2019; Accepted 25 May 2019
Available online 28 May 2019

Table 1
Demographic information on study participants with hemispheric and whole brain group-wise comparisons.

Demographic measures and comparative statistics	0–5 Years	5–10 Years	10–15 Years	15–20 Years
DS mean age (std dev) in years	2.12 (1.25)	7.33 (1.30)	13.78 (0.69)	16.35 (0.86)
Healthy mean age (std dev) in years	2.59 (1.43)	7.63 (1.41)	12.41 (1.41)	16.70 (1.11)
DS age range in years	0.62–4.71	5.17–9.65	12.15–14.86	15.16–17.45
Healthy age range in years	0.00–4.99	5.02–9.98	10.04–14.99	15.01–19.95
DS male/female count	17/9	12/10	10/5	7/2
Healthy male/female count	71/68	124/137	115/177	80/194
Comparative total cortical volume, Cohen's d statistic	−0.62	−0.89	−0.48	−0.17
Comparative left hemisphere mean cortical thickness, Cohen's d statistic	0.53	1.07	1.08	2.57
Comparative right hemisphere mean cortical thickness, Cohen's d statistic	0.44	1.06	0.99	2.46

subsequent cognitive decline (Head et al., 2012; Lott and Head, 2019).

Technological improvements and advancements in medical care have recently led to an increase in lifespans for individuals with DS and an improvement of overall quality of life. Life expectancy of a 1-year old child with DS is estimated to be approximately 53 years of age on average (de Graaf et al., 2017). However, the disorder has not been well studied with modern medical imaging techniques in a clinical setting. We do not know the mechanism by which DS is linked with abnormal brain development and we have not fully characterized the resultant differences in the presentation of the DS brain relative to neurotypical individuals. Further research of DS, including analysis of neurophysiological changes in the brain, can help us better understand the condition and may lead to hypotheses that explain the basis of physiological brain differences in DS.

Magnetic resonance imaging (MRI) provides a wide variety of physiological and anatomical measurements of the brain that may assist in clinical applications as well as basic science research. In the brain, structural MRI provides for the ability to differentiate between white matter, gray matter and cerebrospinal fluid, which forms the basis for the extraction of potentially useful biomarker measurements from various brain regions, such as volume measurements in the white matter, gray matter and ventricles, as well as cortical thickness measurements (e.g. Fischl, 2012).

Neuroimaging studies in DS using MRI have reported increased subcortical gray matter volumes (Pinter et al., 2001) and larger lateral ventricles (Pearlson et al., 1998). Automated MRI brain analysis technologies (e.g. Fischl, 2012) can assess cortical thicknesses in various brain regions. Existing studies investigating the thickness of the cortex in a DS population have produced variable findings, with one recent study reporting increased cortical thickness in DS (Lee et al., 2016) and another recent study reporting decreased cortical thicknesses (Romano et al., 2016) in DS at later ages. The study showing increased cortical thickness (Lee et al., 2016) indicated that the primary regions affected were the frontal, parietal, and occipital lobes. This study also concluded that individuals with DS exhibit a reduced cortical surface area. The study indicating reduced cortical thicknesses in DS (Romano et al., 2016) involved comparison of later years DS participants with neurotypical participants imaged as part of a separate study at a different imaging center. In this study, we hypothesize that assessment of cortical thickness abnormalities (including cortical thickness variability) in DS, including a wider and younger developmental age range and large sample sizes of neurotypical controls, may help improve our understanding of the abnormal neurological development associated with the condition.

2. Materials and methods

2.1. Participants

Following approval by Boston Children's Hospital's (BCH) Institutional Review Board (informed consent was waived due to the lack of risk to participants included in this retrospective analysis), the clinical imaging electronic database at BCH was reviewed for the present analysis from 01/01/2008 until 02/24/2016, and all brain MRI examinations of participants aged 5 to 32 years at the time of imaging were included for further analysis if DS was indicated in the participant's electronic medical records. Examinations deemed to be of low quality (because of excessive participant motion, large metal artefact from a participant's dental hardware, lack of a T1 structural imaging volume providing diagnostically useful axial, sagittal and coronal oriented images etc.) were excluded from this study. Examinations inaccessible for technical reasons were excluded as well. This yielded 47 examinations from participants with DS. The supplementary analysis includes an additional 26 DS examinations from the 0–5 age range. 73% of our DS examinations were from patients with congenital heart defects. Neurotypical participants were assembled retrospectively in a previous analysis (Levman et al., 2017) by selecting participants on the basis of a normal MRI examination, as assessed by a BCH neuroradiologist, and whose medical records provided no indication of any neurological problems (participants with any known disorder were excluded such as autism, cerebral palsy, traumatic brain injury, developmental delay, tuberous sclerosis complex, stroke, neurofibromatosis, epilepsy, attention deficit hyperactivity disorder, etc.). Participants with any form of cancer were also excluded to avoid data exhibiting growth trajectories affected by treatments such as chemotherapy. The same exclusion criteria applied to the DS population was also applied to the neurotypical participants. This yielded 854 examinations, with an additional 139 exams included in the supplementary analysis (ages 0–5 years). Table 1 provides demographic information on participants studied and histograms are provided in Fig. 1.

2.2. MRI Data acquisition and preprocessing

Participants were imaged with clinical 3 Tesla MRI scanners (Skyra, Siemens Medical Systems, Erlangen, Germany) at BCH yielding T1 structural volumetric imaging examinations accessed through the Children's Research and Integration System (Pienaar et al., 2014). The clinical and retrospective nature of this study results in variability in the pulse sequences employed to acquire these volumetric T1 examinations. Strengths and limitations of the large-scale varying MR protocol approach taken in this study are addressed in the paper's Discussion. A single volumetric MRI was acquired from each imaging session and some patients returned for multiple MRI examinations (different imaging sessions) which were used in the analysis. Motion correction was not performed, but examinations with substantial motion artefacts were excluded based on visual assessment. T1 structural examinations were processed with FreeSurfer (Fischl, 2012), using the recon-all command which aligns the input examination to all available brain atlases. Those atlases that include cortical thickness measurements were included for further analysis (atlases: aparc, aparc.a2009, aparc.DKTatlas40, BA, BA.thresh, entorhinal_exvivo). These combined atlases include definitions of 331 cortical regions in the brain from which thickness measurements were extracted. Each FreeSurfer output T1 structural examination was displayed with label map overlays and visually inspected

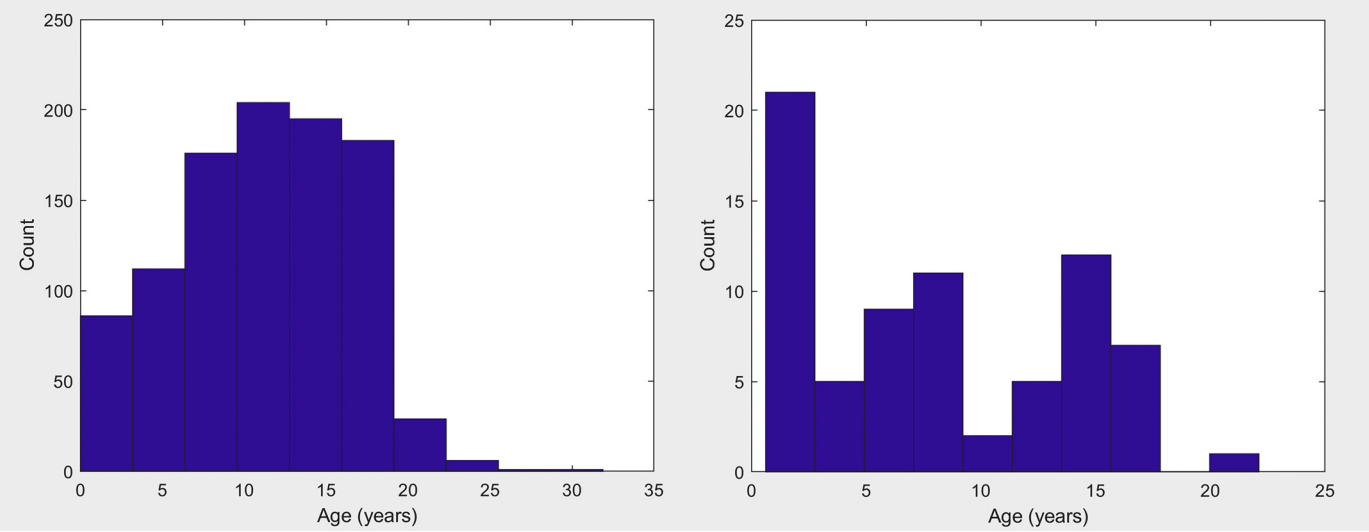

Fig. 1. A histogram of age distributions for our Down Syndrome and neurotypical populations.

for quality of regional segmentation results and exams were excluded from this analysis if FreeSurfer results were observed to substantially fail (i.e. FreeSurfer regions-of-interest (ROIs) that do not align to the MRI and examinations where major problems were observed with an ROI such as a cerebellar segmentation extending far beyond the extent of the cerebellum).

In our DS cohort, this resulted in 1 exam excluded due to a segmentation error, 36 excluded due to technical problems accessing examinations, 65 were excluded due to no volumetric examination available (thus not compatible with FreeSurfer technology), 1 due to no non-contrast enhanced volumetric exam, 1 was excluded due to a motion artefact and 31 examinations were excluded because FreeSurfer failed to complete execution on the patient's exam. In our healthy cohort, 58 were excluded because FreeSurfer failed to complete execution on the patient's exam, 1 due to a major motion artefact, 1 due to an imaging artefact, 231 were excluded due to no volumetric examination, 7 were excluded due to no non-contrast enhanced volumetric exam and 20 were excluded due to technical problems accessing the examinations. As can be seen, the DS group had substantially higher rates of exclusions, which is likely related to the additional challenges in successfully imaging this cohort. The overall rates of motion artefacts are low in both groups, because at our hospital, when motion artefacts are observed by the MR technicians, they repeat an additional structural MRI examination, so imaging sessions produce 1–3 volumetric examinations per patient. One of these was selected for this study for each patient imaging session, based on imaging quality.

2.3. Statistical analysis

This study included the acquisition of 662 regionally distributed cortical thickness measurements per imaging examination, as extracted by FreeSurfer's recon-all command (Fischl, 2012). This included extracting measurements of both the average and the standard deviation of within-region cortical thicknesses for each supported gray matter region. This includes all sub-regions of the brain supporting cortical thickness measurements across all FreeSurfer supported brain atlases. Study participants were divided into three groups based on age: late childhood (5–10 years old), early adolescence (10–15 years old) and late adolescence (15–20 years old). We had very few participants > 20 years old and so did not include them in a separate group, however, all scatter plots included all participants regardless of age to facilitate visual comparison. There is uncertainty regarding the methods employed in this analysis as applied to the youngest patients in our dataset (early childhood: 0–5 years old), and as such all results from this group are relegated to the supplementary materials as a reference. As we were interested in assessing the extent of group-wise differences of these clinically acquired measurements, we compared each measurement (as extracted by FreeSurfer) within each age range in a group-wise manner (DS compared with neurotypical) with Cohen's d statistic (positive/negative values indicate a higher/lower average value in the DS population relative to the neurotypical population). Cohen's d statistic was selected as it is the most established method to assess effect sizes. A *p*-value based on the standard *t*-test (Student, 1908) for two groups of samples was also calculated for each comparison. This yielded a total of $m = 1986$ group-wise comparisons which yielded a Bonferroni corrected threshold for achieving statistical significance of $p < 0.05/m = 2.52e^{-5}$. Supplementary tables present the findings from the 0–5 age group alongside the three older age groups outlined above, yielding $m = 2648$ comparisons included in Tables S1 and S2 with a Bonferroni corrected threshold for achieving statistical significance of $p < 0.05/m = 1.89e^{-5}$.

In order to confirm that the findings reported are the result of group-wise differences between the DS and neurotypical participants, a statistical model was constructed based on multivariate regression (MATLAB R2018a, MathWorks Inc., MA, USA), adjusting each measurement within each age range in order to control for group-wise differences in age, gender and estimated total intracranial volume. This model was used to adjust each cortical thickness measurement (mean and standard deviation), in order to evaluate whether observed group-wise differences between our DS and neurotypical populations are the result of age, gender or intracranial volume effects.

3. Results

Many brain regions showed Bonferroni-corrected, statistically significant differences in cortical thickness measurements between participants with DS and neurotypical controls (average cortical thickness comparisons are provided in Table 2 and comparison of the variability of cortical thicknesses is provided in Table 3). Of the 1986 group-wise comparisons performed, 18.8% were statistically significantly different between DS and control groups after the Bonferroni correction for multiple comparisons, indicating that many brain regions did not exhibit abnormal presentation of cortical thicknesses. All age groupings along with left and right hemisphere results (when available) are provided for ease of comparison. Specifically, there were a large number of regions of the brain exhibiting abnormally increased average cortical thickness as well as abnormally decreased variability of within-region cortical thicknesses. Examples demonstrating the common abnormality

Table 2
Age-dependent analysis – Leading average measurements sorted by effect size (Cohen's d statistic).

Regional cortical measurement of interest	Ages 5–10 years	Ages 10–15 years	Ages 15–20 years
	L (d) R (d)	L (d) R (d)	L (d) R (d)
Brodmann's area 3b MT	L (1.1956) R (1.1805)	L (1.2809) R (1.3318)	L (3.0731) R (2.7298)
Rostral middle frontal MT	L (1.4317) R (1.2794)	L (1.3085) R (1.2761)	L (2.9576) R (2.9847)
Postcentral MT	L (1.4355) R (1.2814)	L (1.4801) R (1.3591)	L (2.9578) R (2.7626)
Medial orbitofrontal MT	L (1.1374) R (0.93384)	L (1.0828) R (0.85334)	L (2.6836) R (1.9296)
Brodmann's area 1 MT	L (1.2729) R (1.3239)	L (1.4378) R (1.5678)	L (2.6583) R (2.5758)
Middle frontal sulcus MT	L (1.3202) R (1.3506)	L (1.0528) R (1.3078)	L (2.5237) R (2.6191)
Whole hemisphere MT	L (1.0686) R (1.0627)	L (1.0754) R (0.99353)	L (2.5713) R (2.4625)
Inferior frontal sulcus MT	L (1.0127) R (1.1016)	L (1.0999) R (1.0048)	L (2.566) R (2.2108)
Orbital gyrus MT	L (0.98257) R (0.77783)	L (0.77274) R (0.75535)	L (2.5657) R (1.7485)
Transverse frontopolar sulci and gyri MT	L (1.0164) R (0.73072)	L (0.7011) R (0.99168)	L (1.925) R (2.5171)
Brodmann's area 45 MT	L (0.94059) R (0.78045)	L (1.0999) R (1.2302)	L (2.4292) R (2.5163)
Brodmann's area 3a MT	L (1.2169) R (0.93797)	L (1.1003) R (1.0689)	L (2.5065) R (2.3258)
Middle frontal gyrus MT	L (1.2166) R (1.0298)	L (1.1787) R (0.91201)	L (2.4436) R (2.4266)
Lateral orbitofrontal MT	L (1.0669) R (0.90833)	L (0.97966) R (1.2639)	L (2.4139) R (2.0683)
Anterior part of the cingulate gyrus and sulcus MT	L (1.1519) R (1.0543)	L (0.84982) R (1.2368)	L (2.1484) R (2.4116)
Brodmann's area 2 MT	L (1.1525) R (1.1971)	L (1.187) R (1.1451)	L (2.388) R (2.3993)
Superior frontal MT	L (1.2723) R (1.2197)	L (1.1713) R (0.9935)	L (2.1985) R (2.3932)
Central sulcus MT	L (1.0735) R (1.0022)	L (0.9821) R (0.88679)	L (2.3838) R (1.812)
Medial occipito-temporal sulcus and lingual sulcus MT	L (0.31273) R (1.1268)	L (0.80358) R (0.48812)	L (2.3824) R (2.123)
Postcentral sulcus MT	L (1.0572) R (1.052)	L (0.96816) R (0.93648)	L (2.3799) R (2.0472)
Marginal branch of the cingulate sulcus MT	L (0.79548) R (0.838)	L (0.91413) R (1.1513)	L (2.3298) R (1.6916)
Pars triangularis MT	L (0.91873) R (0.64676)	L (0.92551) R (0.99841)	L (2.2745) R (2.3047)
Lingual MT	L (1.0323) R (1.0701)	L (1.441) R (1.0273)	L (2.2854) R (1.8872)
Gyrus rectus MT	L (0.49214) R (0.50475)	L (0.57802) R (0.14235)	L (2.272) R (1.1547)
Superior parietal MT	L (1.1939) R (1.0075)	L (1.2331) R (1.1378)	L (2.2686) R (1.951)
Lateral occipital MT	L (0.56727) R (0.91728)	L (0.72711) R (1.0203)	L (1.7653) R (2.2562)

Abbreviations/Symbols: R = right; L = Left; d = Cohen's d statistic, MT = mean thickness.

observed in our dataset of increased mean cortical thickness and decreased cortical thickness variability is provided in Fig. 2 for Brodmann's Area 3b. Fig. 3 demonstrates a FreeSurfer-based (Fischl, 2012) segmentation of the rostral middle frontal region from a DS (right) and a neurotypical participant (left). Note the reduced thickness variability in the individual with DS on the right, a feature that can be hard to visually assess, but for which automated technologies (e.g. Fischl, 2012) can provide relevant measurements.

The age-dependent, d statistic analysis yielded a variety of measurements that may help elucidate the underlying anatomical presentation of the DS brain. Tables 2 and 3 present the leading measurements organized by Cohen's d statistic (highest d values are found at the top of the table). Thus Brodmann's area 3b exhibits the most separation between groups (ages 15–20), the second most separation is

Table 3
Age-dependent analysis – Leading variability measurements (standard deviation of cortical thicknesses) sorted by effect size (Cohen's d statistic).

Regional cortical measurement of interest	Ages 5–10 years	Ages 10–15 years	Ages 15–20 years
	L (d) R (d)	L (d) R (d)	L (d) R (d)
Central sulcus	L (−0.9958) R (−1.041)	L (−0.84813) R (−1.435)	L (−1.6778) R (−1.1025)
Calcarine sulcus	L (−0.86866) R (−1.3461)	L (−0.83957) R (−0.74866)	L (−0.77725) R (−0.83506)
Orbital gyrus	L (−0.51993) R (−0.17382)	L (−0.73376) R (−0.19016)	L (−1.2884) R (−0.96168)
Postcentral	L (−0.98244) R (−0.81665)	L (−0.9326) R (−0.968)	L (−1.2523) R (−0.3002)
Brodmann's area 3b	L (−1.0793) R (−0.4072)	L (−1.0597) R (−0.16356)	L (−1.1328) R (0.55284)
Lateral orbitofrontal	L (−0.35115) R (−0.18625)	L (−1.1173) R (−0.2579)	L (−0.82057) R (−0.29105)
H shaped orbital sulcus	L (−1.0934) R (−0.47677)	L (−0.45479) R (−0.75689)	L (−0.2006) R (0.13329)
Suborbital sulcus	L (−0.4644) R (−0.33238)	L (−0.2653) R (−0.53813)	L (−0.61304) R (−1.0708)
Superior segment of the circular sulcus of the insula	L (−0.43074) R (−0.27873)	L (−0.49151) R (−0.36925)	L (−1.0616) R (−1.0366)
Frontal pole	L (−0.32976) R (−0.62331)	L (−0.77594) R (−0.87523)	L (−1.0045) R (−0.19122)
Planum temporale	L (−0.54804) R (−0.29889)	L (−0.42263) R (−0.80842)	L (−0.016892) R (−0.99533)
Parahippocampal	L (0.29664) R (0.079097)	L (−0.045782) R (−0.19356)	L (−0.98535) R (−0.43674)
Middle temporal gyrus	L (−0.18281) R (−0.49642)	L (−0.34862) R (0.19717)	L (−0.95314) R (−0.46132)
Parahippocampal gyrus	L (−0.010975) R (0.25194)	L (−0.17517) R (−0.26278)	L (−0.94006) R (0.36601)
Inferior segment of the circular sulcus of the insula	L (−0.54792) R (−0.65219)	L (−0.93254) R (−0.81403)	L (−0.035419) R (−0.16179)
Temporal pole	L (−0.38326) R (−0.33081)	L (−0.54762) R (−0.41904)	L (−0.68682) R (−0.92814)
Pars orbitalis	L (−0.87108) R (−0.51568)	L (−0.41826) R (−0.4519)	L (−0.7662) R (−0.75921)
Brodmann's area 4p	L (−0.1098) R (−0.22897)	L (−0.07502) R (−0.74563)	L (−0.86798) R (−0.61679)
Fronto-marginal gyrus and sulcus	L (−0.60447) R (−0.45065)	L (−0.8485) R (−0.14854)	L (−0.50946) R (0.33192)
Posterior ramus of the lateral sulcus	L (−0.43005) R (−0.52486)	L (−0.14436) R (−0.59598)	L (−0.5341) R (−0.84056)
Transverse temporal gyrus	L (−0.016624) R (0.044577)	L (−0.15244) R (−0.15931)	L (−0.82505) R (−0.16424)
Subcallosal gyrus	L (−0.53438) R (−0.4871)	L (−0.807) R (−0.38905)	L (−0.25053) R (0.2401)
Transverse frontopolar gyri and sulci	L (−0.65866) R (−0.23478)	L (−0.31841) R (−0.57919)	L (−0.088659) R (−0.7761)
Insula	L (0.082385) R (−0.10319)	L (−0.46935) R (−0.57684)	L (−0.76821) R (−0.61669)
Lateral aspect of the superior temporal gyrus	L (−0.76016) R (0.016711)	L (−0.34673) R (0.20417)	L (−0.76231) R (−0.017654)

Abbreviations/Symbols: R = right; L = Left; d = Cohen's d statistic.

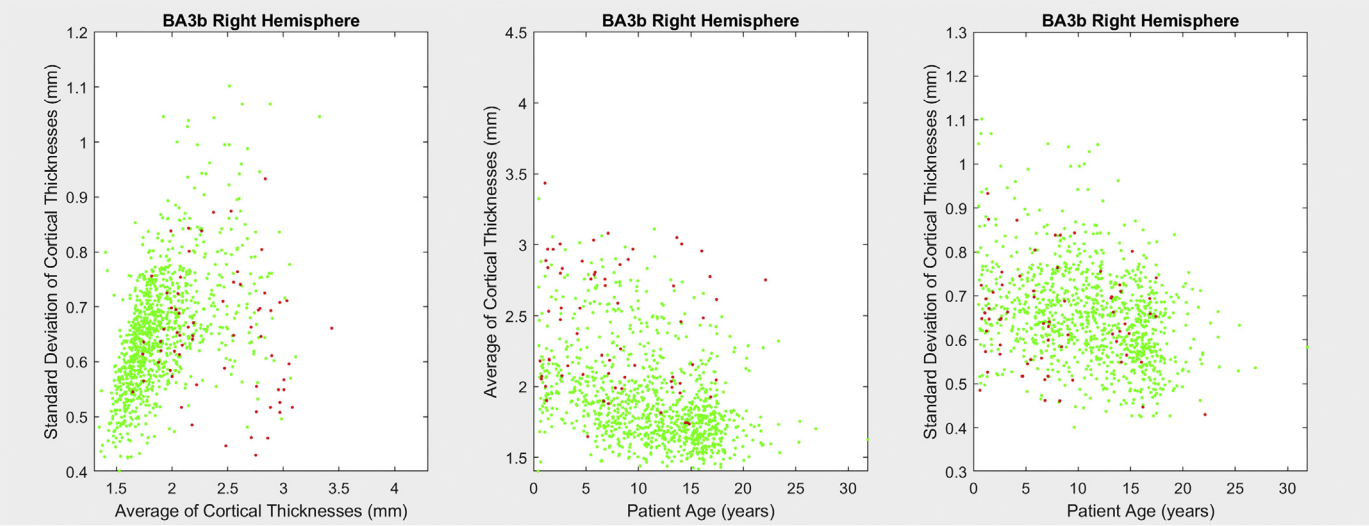

Fig. 2. A scatter plot of Brodmann's Area 3b demonstrating average vs. variability in cortical thickness (left), average cortical thickness vs. age (center) and variability in cortical thickness vs. age (right). Neurotypical participants are represented in green, Down syndrome participants are represented in red. (For interpretation of the references to color in this figure legend, the reader is referred to the web version of this article.)

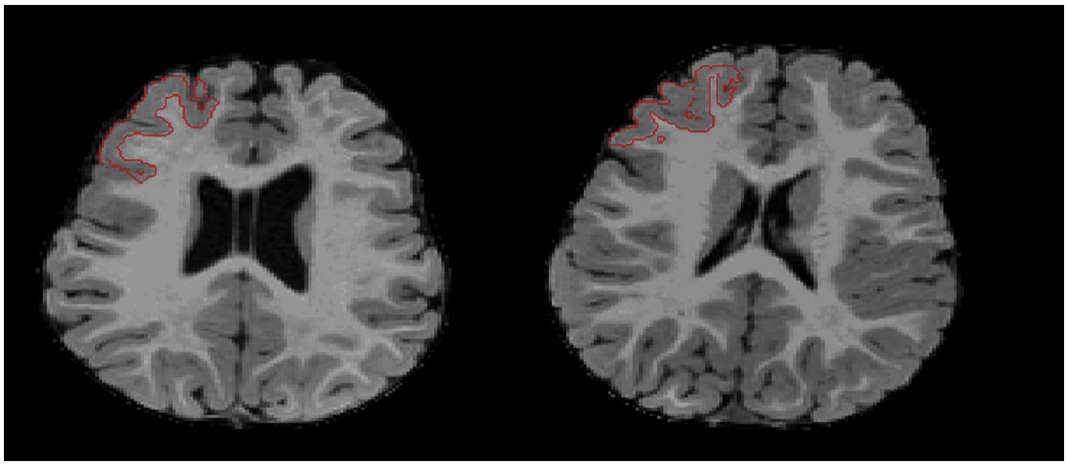

Fig. 3. Example MRI examinations of 13 month old females with Down syndrome (left) and neurotypical (right). The rostral middle frontal region, as established by FreeSurfer, is outlined in red. (For interpretation of the references to color in this figure legend, the reader is referred to the web version of this article.)

found in the rostral middle frontal region (ages 15–20), and so on. We elected to present the raw Cohen's d statistic rather than the adjusted statistic for ease of comparison with future studies. Tables 2 and 3 report overlapping regions of interest including measurements across a region's cortex as well as localized gyral, sulcal and lobular measurements when available. Tables S1 and S2 provide an analysis of the whole range of ages available, including the 0–5 year cohort.

4. Discussion

We performed a large-scale cortical thickness analysis of structural MRI examinations of the brain in DS and neurotypical individuals and demonstrated group-wise differences in average cortical thicknesses as well as cortical thickness variability localized to select regions across the brain. This is the first time regionally focused cortical thickness variability measurements have been reported in the literature for individuals with DS. The observed cortical thickness abnormalities in this study do not affect all brain regions and instead are localized to many sub-regions of the brain (see Tables 2 and 3). Abnormally reduced variability in cortical thickness may be indicative of underlying structural abnormalities prevalent among individuals with DS. Given that both average cortical thicknesses and cortical thickness variability exhibit a nonlinear decreasing trend with age in our neurotypical dataset (visually assessed), increased average thickness and decreased thickness variability implicate abnormal gray matter development in our DS population.

4.1. Relation to literature findings

Age-dependent cortical thinning has been observed repeatedly in healthy populations (Levman et al., 2017), DS (Romano et al., 2016) as well as in our DS population reported in this study (see Fig. 2, middle pane), though to a lesser extent than in our healthy population. Both cortical thickness and variation of regional cortical thickness are recognized as being linked with gyrification (Van Essen, 1997). The degree of cortical gyrification in the first year after birth has a strongly positive correlation with increases in cortical fiber density (Li et al., 2015; Nie et al., 2014), which is associated with the degree of myelination (Dubois et al., 2008) and pruning (Sur and Rubenstein, 2005). Several reports have provided indirect evidence for abnormal pruning in DS patients. DS patients exhibit altered processing of amyloid precursor protein (APP) (Wiseman et al., 2015), which is also observed in Alzheimer's disease, resulting in disrupted axonal pruning and neuronal culling (Kim and Tsai, 2009). DS patients have fewer microglia, which

plays an important role in synaptic pruning (Paolicelli et al., 2011; Xue and Streit, 2011). Additionally, dendritic branching, length and spine density were reported to be increased in a young DS population (Kaufmann and Moser, 2000; Moser, 1999). Pruning dysfunction in DS may play a contributing role in observed thicker cortices relative to our neurotypical population. There is considerable support from the scientific literature for the theory that populations with DS may exhibit irregular pruning. If the theory (presented above) connecting synaptic pruning with cortical thickness is correct, then our findings in this analysis might be indicative of reduced/impaired pruning in the DS population, leading to lessened age-dependent reductions in cortical thicknesses during childhood and adolescence, which was observed in our study in a variety of brain regions (see Tables 2 and 3). Reduced pruning may also give rise to cortical thickness variability abnormalities (see Table 3) depending on the distribution of the location of the sites of pruning within a given cortical subregion.

Our main findings of increased average cortical thicknesses were observed in Brodmann's areas 1 and 3b in the postcentral gyrus and the rostral middle frontal region. Our main findings pertaining to abnormally reduced variability in cortical thicknesses implicate the postcentral gyrus (specifically Brodmann's area 1 and 3b), the lateral orbitofrontal gyri, the orbital gyrus and the central sulcus. The postcentral region, which includes Brodmann's areas 1 and 3b, is the site of the somatosensory cortex, the main sensory area for the sense of touch; abnormalities therein may be linked with observed abnormalities in pain perception among those with DS (Hennequin et al., 2000; McGuire and Defrin, 2015) along with other sensory processing delays (Bruni et al., 2010; Fidler and Nadel, 2007). The lateral orbitofrontal region has been associated with the integration of prior information with current information (Nogueira et al., 2017), and so abnormalities thereof may be linked with intellectual disabilities in DS. The orbital gyrus has been associated with the perception of odors (olfactory senses) and previous research has indicated that participants with DS exhibit severely impaired olfactory function (Cecchini et al., 2016). Abnormally increased cortical thickness of the rostral middle frontal gyrus has been associated with perceived stress (Michalski et al., 2017), and future work can investigate possible associations between cortical thicknesses and neurodevelopmental and psychological outcomes (Walker et al., 2011).

Our study supports the findings of Lee et al., indicating increased cortical thickness in DS. Furthermore, our finding of decreased cortical thickness variability is not contradictory with their findings indicating decreased surface area. When cortical thickness variability is low, the gray matter has fewer folds and curves, resulting in less complicated conformations of the surface of the gyrus which in turn should be associated with decreased surface area. Romano's findings indicating decreased cortical thickness in DS was based on imaging at multiple centers with the DS and neurotypical control groups receiving different imaging protocols, MRI scanners, countries of imaging, age cohorts, and versions of FreeSurfer (Fischl, 2012) to calculate cortical thickness measurements. These inconsistencies between data acquisition and analysis methodologies applied to the two groups of interest may account for the discrepancy between their findings and those presented by Lee and in our study. Differences in the literature may also be attributable to the developmental course of DS, given that Romano's study included much later age ranges (up to 53 years old) than those included in Lee's study and this study.

In the current study, increased cortical thickness in individuals with Down syndrome when compared to neurotypical participants was observed. Our results agree with previous findings (Lee et al., 2016) which showed a statistically significant increase in mean cortical thickness when compared to controls. Although their study did not focus on regions of the brain as small as those considered in our analysis, it concluded that there was an increase in cortical thickness in the frontal, parietal, and occipital lobes. This aligns with the primary areas found in our study, which are located in either the frontal, parietal or occipital lobes. The postcentral gyrus (and the more specific regions: Brodmann's Area 1 and Brodmann's Area 3b) are all located within the parietal lobe. The lingual gyrus is located in the occipital lobe and the rostral middle frontal region and transverse frontopolar sulci and gyri are located in the frontal lobe.

4.2. Strengths & limitations

This study's strengths include a very large cohort of neurotypical participants to compare with those with DS, providing a statistically reliable baseline from which to assess DS related differences. This study also considered intra-regional measurements of cortical thickness variability, making this analysis considerably more thorough than typical cortical thickness studies, which only consider mean values. Our dataset includes many examinations of participants aged 0 to 5 years, providing data on early stages of development that is minimal in the scientific literature, but ambiguity regarding the appropriateness of this study's data processing in this age range remains and so all results from this youngest cohort have been relegated to the supplementary materials as a reference.

Limitations of this study include that it was performed in a clinical environment with pulse sequence variability, though participants were imaged on a consistent set of MRI scanners at Boston Children's Hospital. Strengths and shortcomings of the approach taken in this study have been discussed previously in detail (Levman et al., 2017, 2018). It should be noted that the sample size for the DS group is low, especially in the 10–15 and 15–20 age groups, which have 15 and 9 participants with DS respectively. However, our neurotypical cohort (Levman et al., 2017) is a large population with 993 total examinations, providing a statistically reliable baseline against which to compare our DS population. The small sample size in the later ages may make our findings in these age groups less reliable than those reported for participants under the age of 10 (26 examinations of participants with DS aged 0–5 years and 22 examinations of DS participants aged 5–10 years). Our findings demonstrate a general trend of observing more separation between our DS and neurotypical populations as age increases, however, as age increases our sample size diminishes substantially in our DS population, and so our later age statistics may include considerable measurement variability.

It should also be noted that our analysis is retrospective, thus participants included in our analysis needed to have a reason for being referred to MRI. As such, our analysis may be based on a population with more extreme manifestations of the characteristics of DS, and thus present larger effect sizes than will be obtained in other study designs. It should also be noted that intelligence quotient (IQ) information was unavailable for the participants in this study.

An additional limitation of this study is that the age distributions of available participants in this experiment vary considerably because of the availability of appropriate participants that met our inclusion criteria from a large clinical population. This inevitably resulted in imbalanced pools of participants in our analysis. Our experiment did not involve age- or gender-based participant matching between our DS and neurotypical participants. Instead, we opted to perform our statistical analyses in a group-wise manner, varying the age range under consideration to take advantage of the large sample size available in the neurotypical cohort. This methodology was also selected in order to avoid having our analysis be influenced by the extent of difference between matched pairs of individuals, for which a variety of factors beyond age and gender might influence how appropriate it was for the participants to have been paired (brain volume, sub-structure volume, co-morbidities, etc.). We also performed a multivariate regression analysis that controls for the effects of age, gender and intracranial volume in order to confirm that these factors are not the cause of our reported findings. Comparative assessment of males and females from our neurotypical population revealed no major gender differences in terms of either the mean or the standard deviation of the cortical

thickness measurements (Levman et al., 2017).

An additional limitation of this study is that FreeSurfer (Fischl, 2012) is not optimized for the youngest participants. As such, the rate at which FreeSurfer fails to extract measurements from clinical MRI examinations increases substantially for participants aged 0 to 8 months and the reliability of the results successfully produced by FreeSurfer on participants from this age range is not certain. FreeSurfer's reliability was assessed as reasonable for participants 8-months-old and later (considering this is beyond the age range for which the technology was validated), at which point myelination contrast patterns have inverted so as to match the general pattern exhibited through the rest of life (with gray contrast located on the brain's periphery and white contrast in the brain's central regions). Research aimed at overcoming the problem of FreeSurfer's applicability and reliability in very young populations is ongoing (de Macedo Rodrigues et al., 2015; Zollei et al., 2017) and developments in this venue will be incorporated into future work, which will also involve the extension of this analysis to tractography and functional MRI (fMRI).

An additional limitation is that motion correction was not performed. Instead, we opted to visually inspect each examination and exclude them if image quality was poor. Had motion correction been performed, we may have been able to include additional examinations in the analysis, which may have been affected by sources of error associated with the motion correction algorithm employed. Sedation during image acquisition is common in young patients, however, sedation information was unavailable in this study.

5. Conclusions

In conclusion, our study demonstrated group-wise differences in average cortical thicknesses as well as cortical thickness variability localized to select regions across the brain when comparing Down Syndrome patients with neurotypical controls. This is the first time regionally focused cortical thickness variability abnormalities have been associated with DS. Abnormally reduced variability in cortical thickness may be indicative of underlying structural abnormalities prevalent among patients with DS. Increased average thicknesses and decreased thickness variability implicate abnormal gray matter development in our DS population.

Funding

The authors would like to thank Dr. Henry Feldman, Principal Biostatistician at Boston Children's Hospital for advice on conducting statistical analyses. This work was supported by the National Institutes of Health (grant numbers R01HD078561, R21MH118739, R03NS091587, R21HD098606) to ET; Natural Science and Engineering Research Council of Canada's Canada Research Chair grant (grant number 231266) to JL, Natural Science and Engineering Research Council of Canada Discovery Grant to JL, a Canada Foundation for Innovation and Nova Scotia Research and Innovation Trust infrastructure grant (R0176004) to JL, a St. Francis Xavier University research startup grant to JL (grant number R0168020) and a St. Francis Xavier University UCR grant to JL.

Appendix A. Supplementary data

Supplementary data to this article can be found online at https://doi.org/10.1016/j.nicl.2019.101874.

References

Abbeduto, L., Warren, S.F., Conners, F.A., 2007. Language development in Down syndrome: from the prelinguistic period to the acquisition of literacy. Ment. Retard. Dev. Disabil. Res. Rev. 13, 247–261.

Annus, T., Wilson, L.R., Hong, Y.T., Acosta-Cabronero, J., Fryer, T.D., Cardenas-Blanco, A., Smith, R., Boros, I., Coles, J.P., Aigbirhio, F.I., Menon, D.K., Zaman, S.H., Nestor, P.J., Holland, A.J., 2016. The pattern of amyloid accumulation in the brains of adults with Down syndrome. Alzheimers Dement. 12 (5), 538–545.

Bruni, M., Cameron, D., Dua, S., Noy, S., 2010. Reported sensory processing of children with Down syndrome. Phys. Occup. Ther. Pediatr. 30 (4), 280–293.

Carlesimo, G.A., Marotta, L., Vicari, S., 1997. Long-term memory in mental retardation: evidence for a specific impairment in subjects with Down's syndrome. Neuropsychologia 35, 71–79.

Carr, J., 2005. Stability and change in cognitive ability over the life span: a comparison of populations with and without Down's syndrome. J. Intellect. Disabil. Res. 49, 915–928.

Cecchini, M.P., Viviani, D., Sandri, M., Hahner, A., Hummel, T., Zancanaro, C., 2016. Olfaction in people with Down syndrome: a comprehensive assessment across four decades of age. PLoS ONE 11 (1), e0146486.

Chapman, R.S., Hesketh, L.J., 2001. Language, cognition, and short-term memory in individuals with Down syndrome. Down's Syndr. Res. Pract. J. Sarah Duffen Cent. 7, 1–7.

Couzens, D., Cuskelly, M., Haynes, M., 2011. Cognitive development and Down syndrome: age-related change on the Stanford-Binet test (fourth edition). Am. J. Intellect. Dev. Disabil. 116, 181–204.

de Graaf, G., Buckley, F., Skotko, B.G., 2017. Estimation of the number of people with Down syndrome in the United States. Genet. Med. 19, 439–447.

de Macedo Rodrigues, K., Ben-Avi, E., Sliva, D.D., Choe, M., Drottar, M., Wang, R., Fischl, B., Grant, P.E., Zollei, L., 2015. A FreeSurfer-compliant consistent manual segmentation of infant brains spanning the 0-2 year age range. Front. Hum. Neurosci. 9, 21.

Dubois, J., Dehaene-Lambertz, G., Perrin, M., et al., 2008. Asynchrony of the early maturation of white matter bundles in healthy infants: quantitative landmarks revealed noninvasively by diffusion tensor imaging. Hum. Brain Mapp. 29, 14–27.

Fidler, D.J., Nadel, L., 2007. Education and children with Down syndrome: neuroscience, development, and intervention. Ment. Retard. Dev. Disabil. Res. Rev. 13, 262–271.

Fischl, B., 2012. FreeSurfer. NeuroImage 62 (2), 774–781.

Folin, M., Baiguera, S., Conconi, M.T., Pati, T., Grandi, C., Parnigotto, P.P., Nussdorfer, G.G., 2003. The impact of risk factors of alzheimer's disease in the Down syndrome. Int. J. Mol. Med. 11 (2), 267–270.

Hamlett, E.D., Ledruex, A., Potter, H., Chial, H.J., Patterson, D., Espinosa, J.M., Bettcher, B.M., Granholm, A.C., 2018. Exosomal biomarkers in Down syndrome and Alzheimer's disease. Free Radic. Biol. Med. 114, 110–121.

Head, E., Powell, D., Gold, B.T., Schmitt, F.A., 2012. Alzheimer's disease in Down syndrome. Eur. J. Degener. Dis. 1 (3), 353–364.

Hennequin, M., Morin, C., Feine, J.S., 2000. Pain expression and stimulus localisation in individuals with Down's syndrome. Lancet 356 (9245), 1882–1887.

Jacola, L.M., Byars, A.W., Hicket, F., Vannest, J., Holland, S.K., Schapiro, M.B., 2014. Functional magnetic resonance imaging of story listening in adolescents and young adults with Down syndrome: evidence for atypical neurodevelopment. J. Intellect. Disabil. Res. 58 (10), 892–902.

Jarrold, C., Nadel, L., Vicari, S., 2009. Memory and neuropsychology in Down syndrome. Down Syndr. Res. Pract. 12, 68–73.

Jiang, J., Jing, T., Cost, G.J., Chiang, J.C., Kolpa, H.J., Cotton, A.M., Carone, D.M., Caron, B.R., Shivak, D.A., Guschin, D.Y., Pearl, J.R., Rebar, E.J., Byron, M., Gregory, P.D., Brown, C.J., Urnov, F.D., Hall, L.L., Lawrence, J.B., 2013. Translating dosage compensation to trisomy 21. Nature 500 (7462), 296–300.

Kaufmann, W., Moser, H.W., 2000. Dendritic anomalies in disorders associated with mental retardation. Cereb. Cortex 10 (10), 981–991.

Kim, D., Tsai, L.H., 2009. Bridging physiology and pathology in AD. Cell 137 (6), 997–1000.

Lao, P.J., Handen, B.L., Betthauser, T.J., Mihalia, I., Hartley, S.L., Cohen, A.D., Tudorascu, D.L., Bulova, P.D., Lopresti, B.J., Tumuluru, R.V., Murali, D., Mathis, C.A., Barnhart, T.E., Stone, C.K., Price, J.C., Devenny, D.A., Mailick, M.R., Klunck, W.E., Johnson, S.C., Christian, B.T., 2017. Longitudinal changes in amyloid positron emission tomography and volumetric magnetic resonance imaging in the nondemented Down syndrome population. Alzheimers Dement. 9, 1–9.

Lee, N.R., Adeyemi, E.I., Lin, A., Clasen, L.S., Lalonde, F.M., Condon, E., Driver, D.I., Shaw, P., Gogtay, N., Raznahan, A., Giedd, J.N., 2016. Dissociations in cortical morphometry in youth with Down syndrome: evidence for reduced surface area but increased thickness. Cereb. Cortex 26 (7), 2982–2990.

Letourneau, A., Santoni, F.A., Bonilla, X., Sailani, M.R., Gonzalez, D., Kind, J., Chevalier, C., Thurman, R., Sandstorm, R.S., Hibaoui, Y., Garieri, M., Popadin, J., Falconnet, E., Gagnebin, M., Gehrig, C., Vannier, A., Guipponi, M., Farinelli, L., Robyr, D., Migliavacca, G., Borel, C., Deutsch, S., Feki, A., Stamatoyannopoulos, J.A., Herault, Y., Steensel, B.V., Guigo, R., Antonarakis, S.E., 2014. Domains of genome-wide gene expression dysregulation in Down's regulation. Nature 531 (7594), 345–350.

Levman, J., MacDonald, P., Lim, A.R., Forgeron, C., Takahashi, E., 2017. A pediatric structural MRI analysis of healthy brain development from newborns to young adults. Hum. Brain Mapp. 38 (12), 5931–5942.

Levman, J., Vasung, L., MacDonald, P., Rowley, S., Stewart, N., Lim, A.R., Ewenson, B., Galaburda, A., Takahashi, E., 2018. Regional volumetric abnormalities in pediatric autism revealed by structural magnetic resonance imaging. Int. J. Dev. Neurosci. 71, 34–45.

Li, G., Liu, T., Ni, D., Lin, W., Gilmore, J.H., Shen, D., 2015. Spatiotemporal patterns of cortical fiber density in developing infants, and their relationship with cortical thickness. Hum. Brain Mapp. 36, 5183–5195.

Lott, I.T., Head, E., 2019. Dementia in Down syndrome: unique insights for Alzheimer disease research. Nat. Rev. Neurol. 15 (3), 135–147.

Lowry, R.B., Jones, D.C., Renwick, D.H.G., Trimble, B.K., 1976. Down syndrome in British Columbia, 1952-73: incidence and mean maternal age. Genet. Cytogenet. 14 (1), 29–34.

McGuire, B.E., Defrin, R., 2015. Pain perception in people with Down syndrome: a synthesis of clinical and experimental research. Front. Behav. Neurosci. 9, 194.
Michalski, L.J., Demers, C.H., Baranger, D.A.A., Barch, D.M., Harms, M.P., Burgess, G.C., Bogdan, R., 2017. Perceived stress is associated with increased rostral middle frontal gyrus cortical thickness: a family-based and discordant-sibling investigation. Genes Brain Behav. 16 (8), 781–789.
Moser, H.W., 1999. Dendritic anomalies in disorders associated with mental retardation. Dev. Neuropsychol. 16 (3), 369–371.
Nie, J., Li, G., Wang, L., et al., 2014. Longitudinal development of cortical thickness, folding, and fiber density networks in the first 2 years of life. Hum. Brain Mapp. 35, 3726–3737.
Nielsen, J., Sillesen, I., 1975. Incidence of chromosome aberrations among 11 148 newborn children. Humangenetik 30 (1), 1–12.
Nogueira, R., Abolafia, J.M., Drugowitsch, J., Balaguer-Ballester, E., Sanchez-Vives, M.V., Moreno-Bote, R., 2017. Lateral orbitofrontal cortex anticipates choices and integrates prior with current information. Nat. Commun. 8, 14823.
Paolicelli, R.C., Bolasco, G., Pagani, F., Maggi, M., Scianni, M., Panzanelli, P., Giustetto, M., Ferreira, T.A., Guiducci, E., Dumas, L., Ragozzino, D., Gross, C.T., 2011. Synaptic pruning by microglia is necessary for normal brain development. Science 333, 1456–1458.
Pearlson, G.D., Breiter, S.N., Aylward, E.H., Warren, A.C., Grygorcewicz, M., Frangou, S., Barta, P.E., Pulsifer, M.B., 1998. MRI brain changes in subjects with Down syndrome with and without dementia. Dev. Med. Child Neurol. 40 (5), 326–334.
Pienaar, R., Rannou, N., Haehn, D., Grant, P.E., 2014. ChRIS: Real-time web-based MRI data collection analysis, and sharing. In: 20th Annual Meeting of the Organization for Human Brain Mapping. vol. 5.
Pinter, J.D., Eliez, S., Schmitt, J.E., Capone, G.T., Reiss, A.L., 2001. Neuroanatomy of Down's syndrome: a high resolution MRI study. Am. J. Psychiatry 158 (10), 1659–1665.
Rafii, M.S., Lukic, A.S., Andrews, R.D., Brewer, J., Rissman, R.A., Strother, S.C., Wernick, M.N., Pennington, C., Mobley, W.C., Ness, S., Matthews, D.C., Down Syndrome Biomarker Initivative and the Alzheimer's Disease Neuroimaging Initiative, 2017. PET imaging of tau pathology and relationship to amyloid, longitudinal MRI, and cognitive change in Down syndrome: results from the Down syndrome biomarker initiative(DSBI). J. Alzheimers Dis. 60 (2), 439–450.
Raha-Chowdhury, R., Henderson, J.W., Raha, A.A., Stott, S.R.W., Vuono, R., Foscarin, S., Wilson, L., Annus, T., Fincham, R., Allinson, K., Devalia, V., Freidland, R.P., Holland, A., Zaman, S.H., 2018. Erythromyeloid-derived TREM2: a major determinant of Alzheimer's disease pathology in Down syndrome. J. Alzeheimer's Dis. 61 (3), 1143–1162.
Romano, A., Cornia, R., Moraschi, M., Bozzao, A., Chiacchiararelli, L., Coppola, V., Iani, C., Stella, G., Albertini, G., Pierallini, A., 2016. Age-related cortical thickness reduction in non-demented down's syndrome subjects. J. Neuroimaging 26 (1), 95–102.
Sherman, S.L., Allen, E.G., Bean, L.H., Freeman, S.B., 2007. Epidemiology of Down syndrome. Ment. Retard. Dev. Disabil. Res. Rev. 13 (3), 221–227.
Silverman, W., 2007. Down syndrome: cognitive phenotype. Ment. Retard. Dev. Disabil. Res. Rev. 13, 228–236.
Student, S., 1908. The probable error of a mean. Biometrika 6 (1), 1–25.
Sur, M., Rubenstein, J.L., 2005. Patterning and plasticity of the cerebral cortex. Science 310, 805–810.
Van Essen, D.C., 1997. A tension-based theory of morphogenesis and compact wiring in the central nervous system. Nature 385, 313–318.
Walker, J.C., Dosen, A., Buitelaar, J.K., Janzing, J.G., 2011. Depression in Down syndrome: a review of the literature. Res. Dev. Disabil. 32 (5), 1432–1440.
Wan, Y.T., Chiang, C.S., Chen, S.C., Wuang, Y.P., 2017. The effectiveness of the computerized visual perceptual training program on individuals with Down syndrome: an fMRI study. Res. Dev. Disabil. 66, 1–5.
Wiseman, F.K., Al-Janabi, T., Hardy, J., et al., 2015. A genetic cause of Alzheimer disease: mechanistic insights from Down syndrome. Nat. Rev. Neurosci. 16, 564–574.
Xue, Q.S., Streit, W.J., 2011. Microglial pathology in Down syndrome. Acta Neuropathol. 122, 455–466.
Zollei, L., Ou, Y., Iglesias, J., Grant, P.E., Fischl, B., 2017. FreeSurfer image processing pipeline for infant clinical MRI images. In: Proceedings of the Organization for Human Brain Mapping Conference. vol. 1703 (Vancouver, BC, Canada).